Acta Biochim Biophys Sin 2023, 55(5): 736–748
https://doi.org/10.3724/abbs.2023081
Advance Access Publication Date: 11 May 2023
Original Article

Original Article

Coaggregation of polyglutamine (polyQ) proteins is mediated by polyQ-tract interactions and impairs cellular proteostasis

Jun-Ye Hong[1,2,†], Jian-Yang Wang[1,2,†], Hong-Wei Yue[1,2], Xiang-Le Zhang[1,2], Shu-Xian Zhang[1,2], Lei-Lei Jiang[1], and Hong-Yu Hu[1,*]

[1]State Key Laboratory of Molecular Biology, Shanghai Institute of Biochemistry and Cell Biology, Center for Excellence in Molecular Cell Science, Chinese Academy of Sciences, Shanghai 200031, China, and [2]University of Chinese Academy of Sciences, Beijing 100049, China
[†]These authors contributed equally to this work.
*Correspondence address. Tel: +86-21-54921121; E-mail: hyhu@sibcb.ac.cn

Received 13 October 2022 Accepted 25 November 2022

Abstract

Nine polyglutamine (polyQ) proteins have already been identified that are considered to be associated with the pathologies of neurodegenerative disorders called polyQ diseases, but whether these polyQ proteins mutually interact and synergize in proteinopathies remains to be elucidated. In this study, 4 polyQ-containing proteins, androgen receptor (AR), ataxin-7 (Atx7), huntingtin (Htt) and ataxin-3 (Atx3), are used as model molecules to investigate their heterologous coaggregation and consequent impact on cellular proteostasis. Our data indicate that the N-terminal fragment of polyQ-expanded (PQE) Atx7 or Htt can coaggregate with and sequester AR and Atx3 into insoluble aggregates or inclusions through their respective polyQ tracts. *In vitro* coprecipitation and NMR titration experiments suggest that this specific coaggregation depends on polyQ lengths and is probably mediated by polyQ-tract interactions. Luciferase reporter assay shows that these coaggregation and sequestration effects can deplete the cellular availability of AR and consequently impair its transactivation function. This study provides valid evidence supporting the viewpoint that coaggregation of polyQ proteins is mediated by polyQ-tract interactions and benefits our understanding of the molecular mechanism underlying the accumulation of different polyQ proteins in inclusions and their copathological causes of polyQ diseases.

Key words polyglutamine, coaggregation, protein interaction, proteostasis, sequestration

Introduction

Protein misfolding and aggregation are generally considered the common pathological causes of some neurodegenerative diseases (NDs) [1,2]. To date, nine NDs have been identified that are caused by proteins with a polyglutamine (polyQ) tract in their sequences [3], and these disorders are collectively referred to as polyQ diseases [4,5]. In general, patients with polyQ diseases will have neuronal loss and share similar symptoms with movement disorders [5]. Expansion of the polyQ tracts encoded by aberrantly expanded *CAG* repeats will lead to protein aggregation and consequently cause diseases [6–10]. Accumulating evidence suggests a recruitment/sequestration hypothesis in which the aggregates formed by a polyQ protein sequester essential cellular partners (proteins and/or RNA) and thus cause the functional loss of these partners, which may contribute to disease pathologies [11–17].

According to the specific protein-interaction features, four types of protein sequestration have been characterized and classified: protein coaggregation, domain/motif-mediated sequestration, RNA-assisted sequestration, and sequestration of molecular chaperones [16,18]. Among these, coaggregation is generally taken up by two or more amyloidogenic proteins, which can be homologous or heterologous. A pathogenic protein or its variant (usually derived from mutation or fragmentation) coaggregates mutually and sequesters its own wild-type (WT) or full-length protein or other heterologous proteins. For instance, P53 is a crucial protein that regulates the cell cycle and hence functions as a tumor suppressor; some types of P53 mutants are prone to aggregation and coaggregate with WT P53 [19–21] or other multiple tumor suppressors, such as P63 and P73 [22], resulting in functional loss of the tumor suppressors.

For polyQ proteins, proteolytic cleavage is considered a critical step in triggering protein aggregation and disease occurrence [23–27]. The

N-terminal fragments of polyQ-expanded (PQE) huntingtin (Htt) [28–30] and ataxin-7 (Atx7) [31–33] have been identified and well characterized. The C-terminal polyQ-containing fragments of ataxin-3 (Atx3) were also reported to be pathogenic [34–37], and these fragments readily aggregate and sequester full-length Atx3 into amyloid-like aggregates in cells [14,34]. Androgen receptor (AR), another polyQ protein, is a steroid hormone ligand-activated transcription factor related to sex differentiation and bone and muscle development [38,39]. Upon binding with androgen, AR can target androgen responsive elements (AREs) and activate the transcription of downstream genes with the help of coactivators [40]. In a yeast model, the N-terminal polyQ-containing fragments of AR can interact with the full-length protein and inhibit its transactivation function [41]. Apart from sequestration of the full-length polyQ proteins by their toxic fragments, coaggregation also occurs among these heterologous proteins that each contain a polyQ tract. For example, TATA-binding protein (TBP), a transcription factor containing a pathogenic polyQ tract, was found to be sequestered by the aggregates formed by Htt in patient brains or by Atx3 in a cell model [14]. CREB-binding protein (CBP), another polyQ-containing transcriptional coactivator, can coaggregate with several PQE proteins, such as Htt [42,43] and Atx3 [44–46]. These coaggregation and sequestration processes may cause depletion of CBP and thereby neurotoxicity [17].

As reported in the literature, coaggregation of polyQ proteins and their variants in cells or brains is implicit in the proteinopathies of polyQ diseases [14,34,42,44,47]. A PQE protein fragment can coaggregate with other polyQ-containing proteins and sequester them into amyloid-like aggregates. However, how these proteins mutually coaggregate and sequester each other and how polyQ aggregates induce neuronal cytotoxicity and degeneration remain contentious.

In the present study, to address the molecular mechanism underlying the coaggregation of polyQ proteins, we applied four polyQ-containing proteins (AR, Atx7, Htt and Atx3) as well as ataxin-2 (Atx2) [48] as model molecules and found that the N-terminal fragment of PQE Atx7 or Htt can sequester AR and Atx3 into insoluble aggregates through direct protein interactions among their polyQ tracts. Moreover, these coaggregation and sequestration effects may interfere with the transactivation function of AR. This study will benefit our understanding of why heterologous polyQ proteins appear in the accumulation of the inclusion bodies formed by a specific polyQ-expanded protein.

Materials and Methods

Plasmids, antibodies and reagents

All the plasmids applied for this study are listed in Supplementary Table S1. Taking $Atx7_{10Q}$-N172 as an example for nomenclature of the constructs, the N-terminal 172 residues of ataxin-7 have 10 successive glutamines. For eukaryotic expression, the cDNAs encoding Atx7-N172 (N-terminal residues 1–172 of Atx7), Htt-N90 (N-terminal residues 1–90), Htt-N552 (N-terminal residues 1–552) and their PQE variants were cloned into a FLAG-pcDNA3.0 vector, while full-length AR, Atx3-I (isoform-I) and Atx2-N317 (N-terminal residues 1–317) species with different polyQ lengths were cloned into an HA-pcDNA3.0. For prokaryotic expression, the cDNAs encoding Atx7-N62 (N-terminal residues 1–62) and its variants were cloned into a pET-32 M vector (with a Trx domain fused in the N-terminus) [49]. The cDNAs for Atx3-IIC species (isoform-II, residues 221–373) of 6Q and 22Q were cloned into pET-22b, while that for 46Q was cloned into a pGBTNH vector (with a GB1 domain fused in the N-terminus) [50].

The anti-FLAG and anti-HA antibodies were purchased from Sigma (St Louis, USA), and the antibodies against AR, Atx3 or GAPDH were from Santa Cruz (Santa Cruz, USA), Abclonal (Boston, USA) and Proteintech (Wuhan, China), respectively. All secondary antibodies were obtained from Jackson ImmunoResearch Laboratories (West Grove, USA). Polyvinylidene fluoride (PVDF) membranes were purchased from PerkinElmer Life Sciences (Boston, USA), and an ECL detection kit was purchased from Thermo Scientific (Waltham, USA).

Cell culture and transfection

HEK 293T cells were cultured in DMEM (HyClone, Carlsbad, USA) supplemented with 10% fetal bovine serum (Gemini, New York, USA) and penicillin and streptomycin at 37°C under a humidified atmosphere containing 5% CO_2. Transfection of plasmids in HEK 293T cells was performed by using PolyJet reagent (SignaGen, Jinan, China) according to the manufacturer's instructions.

Supernatant/pellet fractionation

HEK 293T cells transfected with specific plasmids were lysed using 100 μL RIPA buffer (50 mM Tris-HCl, pH 7.5, 150 mM NaCl, 1 mM EDTA, 1% NP-40, and cocktail protease inhibitor) on ice for 30 min and centrifuged at 16,200 *g* for 15 min at 4°C. The supernatant fraction was added to 100 μL of 2 × loading buffer (2% SDS), while the pellet was washed with RIPA buffer 3 times (16,200 *g*, 3 min) and then added to 40 μL of 4 × loading buffer (2% SDS) [51].

Western blot and statistical analysis

The samples were subject to SDS-PAGE (12% or 15% gel) and transferred onto PVDF membranes using the wet transfer method. The proteins were detected by using specific primary and secondary antibodies and the ECL detection kit. Protein bands in gels were scanned with ImageJ software, and their gray values were obtained from the integrated band areas. Thus, the relative amount of each protein could be quantified relative to that of the control. The data from three independent experiments were further analyzed statistically by OriginPro software using one-way ANOVA. The protein level is presented as the mean ± SEM ($n = 3$). The P values in the graphs are labelled with * ($P < 0.05$), ** ($P < 0.01$), *** ($P < 0.001$) and N.S. (no significance), respectively.

Immunofluorescence microscopy

HEK293T cells were transfected with each plasmid as described previously [51]. Approximately 48 h after transfection, the cells were fixed with 4% paraformaldehyde for 15 min, permeabilized with 0.1% Triton X-100 and blocked with a blocking solution (5% BSA and 10% FBS in PBS buffer) for 1 h. After blocking, the cells were incubated with the respective primary antibodies against FLAG (1:100) and AR (1:100) for 3 h at room temperature or overnight at 4°C. After being washed 3 times with PBS buffer, the cells were labelled with FITC-conjugated anti-mouse (1:100) and TRITC-conjugated anti-rabbit (1:100) antibodies (Jackson ImmunoResearch Laboratories) for 1 h. The cell nuclei were stained with Hoechst (Sigma). The cells were visualized on a Leica Microsystems TCS SP8 confocal microscope (Wetzlar, Germany).

Luciferase reporter assay

The pGL3-ARE plasmid was constructed based on the luciferase

reporter vector pGL3 (Promega, Madison, USA). A DNA fragment with three tandem ARE repeats (ARE sequence: 5′-agaacagcaagtgct-3′) was inserted into the *Sac*I and *Xho*I sites upstream of the promoter-luc$^+$ transcriptional unit [52,53]. The luciferase reporter assay was carried out using a Luciferase Reporter Assay kit (Yeasen Biotech, Shanghai, China) according to the manufacturer's protocol [54]. Briefly, FLAG-tagged Atx7-N172 (10Q, 93Q) or Htt-N552 (18Q, 100Q) and pGL3-ARE were cotransfected into HEK 293T cells. To verify the transactivation function of endogenous AR, DHT (Wuxi AppTec, Wuxi, China) dissolved in absolute ethanol was also included in the cell culture (1 nM) to repeat the experiment. Approximately 48 h after transfection, the cells were treated with 500 μL of lysis buffer for 15 min at room temperature, and the lysates were centrifuged at 13,000 rpm for 5 min to remove any precipitates. Then, 100 μL of the supernatant was taken and mixed with 100 μL of the detection reagent, and the fluorescence intensity was detected on a microplate reader (Synergy NEO; BioTek, Vermont, USA).

Protein expression and purification

All proteins were overexpressed in the *Escherichia coli* BL21 (DE3) strain (Invitrogen, Carlsbad, USA). All proteins were fused with a His6-tag and initially purified by a Ni^{2+}-NTA column (Roche, Basel, Switzerland), followed by size-exclusion chromatography (Superdex-200; GE Healthcare, Wisconsin, USA). The Trx tag of Atx7-N62 or GB1 tag of $Atx3_{46Q}$-IIC was removed by thrombin digestion and a second Ni^{2+}-NTA column. The protein concentration was determined by using the BCA Protein Assay kit (Sangon, Shanghai, China).

In vitro coprecipitation experiment

The coprecipitation experiments were performed in PBS buffer (50 mM phosphate, 50 mM NaCl, pH 7.0) [50]. The stock concentrations of $Atx3_{6Q}$-IIC, $Atx3_{22Q}$-IIC and $Atx7_{33Q}$-N62 were 100 μM. The $Atx7_{33Q}$-N62 protein was mixed with $Atx3_{6Q}$-IIC or $Atx3_{22Q}$-IIC at different molar ratios, and NaN_3 (0.004%; w/v) was included in the mixture to prevent the growth of bacteria. The protein mixtures were incubated at room temperature for 24 h or 48 h, followed by supernatant/pellet fractionation.

NMR titration experiment

The labelling and purification of ^{15}N-$Atx7_{22Q}$-N62 and $Atx3_{22Q}$-IIC were carried out according to our previous work [49,50]. The ^{1}H-^{15}N HSQC spectra were recorded on a Bruker 900-MHz NMR spectrometer (Bruker, Billerica, USA) at 298 K, and the ^{1}H and ^{15}N chemical shifts of $Atx7_{22Q}$-N62(T3N9) (BMRB No. 27335) were followed with its backbone assignments completed previously [49]. All titrations were in PBS buffer (20 mM phosphate, and 50mM NaCl, pH 6.5), and the concentration of ^{15}N-labelled $Atx7_{22Q}$-N62(T3N9) was 100 μM. The ratios of $Atx7_{22Q}$-N62/$Atx3_{22Q}$-IIC were set at 1:0, 1:0.5, 1:1 and 1:2. The NMR data were processed by NMRpipe, and the peaks were marked and analyzed with Sparky. The peak heights were normalized to that of the ^{15}N-labelled $Atx7_{22Q}$-N62 only (ratio 1:0).

Results

PQE protein fragments can sequester endogenous AR and Atx3 into insoluble aggregates

PolyQ proteins are diverse in structure and function, but accumulating evidence implies that they can coaggregate with each other. To determine whether polyQ proteins, such as AR and Atx3, could be sequestered by other PQE proteins apart from being recruited by their own fragments, four polyQ proteins or fragments (Atx7-N172, Htt-N552 or Htt-N90, AR and Atx3) were used for our studies. We first examined whether the PQE protein fragments redistribute endogenous AR and Atx3 into insoluble aggregates in cells. We transfected $Atx7_{10Q}$-N172 and $Atx7_{93Q}$-N172 into HEK 293T cells and separated the supernatant and pellet fractions of AR and Atx3 proteins. The data showed that upon transfection with $Atx7_{93Q}$-N172, the protein level of AR in the supernatant fraction was decreased significantly compared with transfection with $Atx7_{10Q}$-N172 (normal polyQ length), whereas that in the pellet was increased remarkably (Figure 1A,B). A similar result was also obtained for endogenous Atx3, which could be sequestered into the insoluble fraction (Figure 1C,D). This observation indicates that both endogenous AR and Atx3 can be sequestered into insoluble aggregates or inclusions by the N-terminal fragment of PQE Atx7. We also examined Htt_{100Q}-N552 for the sequestration effect and found a similar ability to $Atx7_{93Q}$-N172 to sequester endogenous AR and Atx3 into insoluble aggregates (Figure 2). Together, the expression of a PQE protein or fragment is able to sequester another polyQ protein into insoluble aggregates in cells.

To exclude the possibility that conjugated ubiquitin (Ub) may interact with Atx3 and cause coaggregation of the PQE protein with Atx3 [55], we applied a mutant of Htt_{100Q}-N90 (3KR, three Lys residues replaced by Arg) for the experiment as described previously [51]. We found that, similar to WT Htt_{100Q}-N90, its 3KR mutant could also coaggregate with endogenous Atx3 and sequester it into aggregates, indicating that the coaggregation does not originate from conjugated Ub binding with the UIM domains of Atx3. Thus, the N-terminal fragment of PQE Atx7 or Htt can sequester endogenous AR and Atx3 into aggregates via a coaggregation process.

To ensure that the colocalization between $Atx7_{93Q}$-N172 and AR does exist in cells, we visualized the cellular localization of AR in the $Atx7_{93Q}$-N172 inclusions by confocal microscopy. The images showed that endogenous AR was well colocalized with the cytoplasmic inclusions formed by $Atx7_{93Q}$-N172 (Figure 3), whereas the AR molecules were dispersed in cells without overexpression of the PQE fragment. A similar result was also observed in endogenous Atx3, in which most Atx3 molecules showed preferential localization in the nucleus, while some were colocalized with the nuclear inclusions formed by a nuclear species of $Atx7_{93Q}$-N172. Overall, endogenous polyQ-containing proteins, such as AR and Atx3, can be sequestered into insoluble aggregates or inclusions formed by PQE protein fragments in cells, which might contribute to the proteinopathies of proteolytic fragments from polyQ proteins.

The PQE fragments also sequester exogenous AR and Atx3

To further corroborate the sequestration effects of AR and Atx3 by the PQE protein fragments, we cotransfected HA-tagged AR or Atx3 with FLAG-Atx7-N172 (10Q, 93Q) into HEK 293T cells and performed supernatant/pellet fractionation. As expected, both exogenous AR (23Q) (Figure 4A,B) and Atx3 (22Q) (Figure 4C,D) were efficiently sequestered into aggregates by $Atx7_{93Q}$-N172 but not by $Atx7_{10Q}$-N172. Thus, the N-terminal fragment of PQE Atx7 also has a strong ability to sequester exogenous AR and Atx3 into

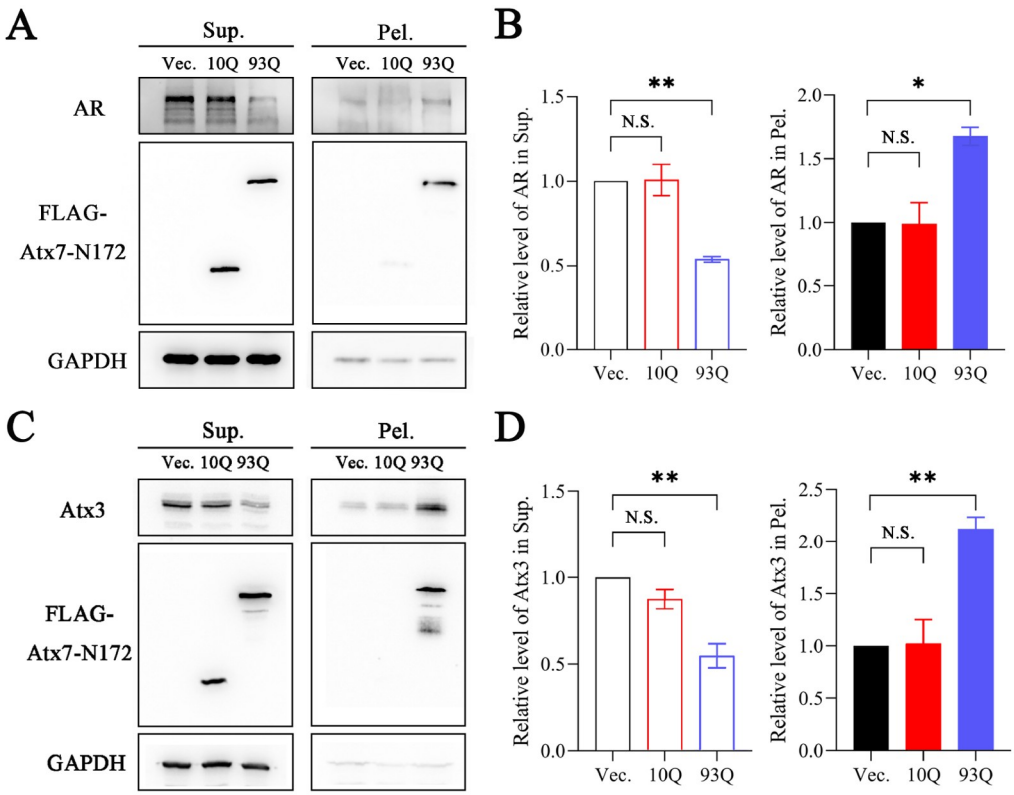

Figure 1. The PQE Atx7 fragment sequesters endogenous AR and Atx3 into insoluble aggregates (A,C) Supernatant/pellet fractionation for detecting sequestration of endogenous AR (A) and Atx3 (C) by $Atx7_{93Q}$-N172. HEK 293T cells were transfected with empty vector, FLAG-$Atx7_{10Q}$-N172 or FLAG-$Atx7_{93Q}$-N172. Approximately 48 h after transfection, the cell lysates were subject to supernatant/pellet fractionation and then to western blot analysis with an anti-FLAG, anti-AR or anti-Atx3 antibody. (B,D) Quantification of the protein levels of AR (B) and Atx3 (D) in supernatant and pellet fractions. Data are shown as the mean ± SEM ($n = 3$). *$P < 0.05$; **$P < 0.01$; N.S., no significance. Vec., vector; Sup., supernatant; Pel., pellet.

insoluble aggregates. Collectively, all the results from AR and Atx3 imply that a PQE protein can sequester other polyQ-containing proteins in cells via coaggregation of the heterologous polyQ proteins.

The polyQ tract plays an important role in coaggregation

Atx7 and AR are two nonhomologous proteins that are not structurally and functionally related, and there is currently no evidence to prove that they directly interact with other regions outside the polyQ tracts. Our supernatant/pellet fractionation and immunofluorescence images confirmed that the fragment of PQE Atx7 or Htt can sequester AR and Atx3 into aggregates in cells. Therefore, we assumed that coaggregation may occur between the two proteins through their respective polyQ tracts. To test this hypothesis, we prepared polyQ-shortened variants that may attenuate or disrupt the polyQ-polyQ interaction and re-examined their sequestration effect. The results showed that, compared with normal AR (23Q), the AR variants with shorter polyQ lengths (10Q, 3Q) had decreased protein levels in the pellet fractions, whether in the presence or absence of $Atx7_{93Q}$-N172 (Figure 5). Notably, there were considerable amounts of any AR forms in the pellet, possibly due to self-aggregation of the full-length AR. It seemed that shortening the polyQ tract could also reduce the AR aggregates, but the amount of each AR form in the pellet precipitated by $Atx7_{93Q}$-N172 was much larger than that of the respective AR only. AR is a large protein; it may have basal aggregation regardless of the polyQ tract. Therefore, we resorted to the N-terminal fragment of Atx2 (Atx2-N317, residues 1–317) to clarify the uncertainty. We cotransfected FLAG-$Atx7_{93Q}$-N172 and various HA-tagged Atx2-N317 species (23Q, 9Q, 3Q) into HEK 293T cells and performed supernatant/pellet fractionation. With the shortening of the polyQ sequence, the amount of Atx2-N317 precipitated by $Atx7_{93Q}$-N172 decreased significantly, whereas the basal aggregation of Atx2-N317 had only a small variation (Figure 6). Similarly, the amount of each Atx2-N317 form sequestered by $Atx7_{93Q}$-N172 was much larger than that from its basal aggregation. Taken together, shortening of the polyQ tract can effectively reduce the ability of AR and Atx2-N317 to be sequestered by $Atx7_{93Q}$-N172, indicating that synergistic coaggregation occurs between the polyQ proteins and that polyQ-tract interactions may play a role in coaggregation and sequestration.

Coaggregation of polyQ proteins *in vitro*

To validate the above observation, we investigated the coaggregation effect of the polyQ proteins *in vitro*. We first purified two polyQ-containing protein fragments, $Atx7_{33Q}$-N62 (N-terminal fragment of Atx7, residues 1–62) [49] and Atx3-IIC (C-terminal fragment of isoform-II Atx3, residues 221–373), with different polyQ lengths (22Q and 6Q) [50] and then performed coprecipitation experiments on the incubation mixtures of $Atx7_{33Q}$-N62 and normal (22Q) or polyQ-shortened (6Q) Atx3-IIC by separating the

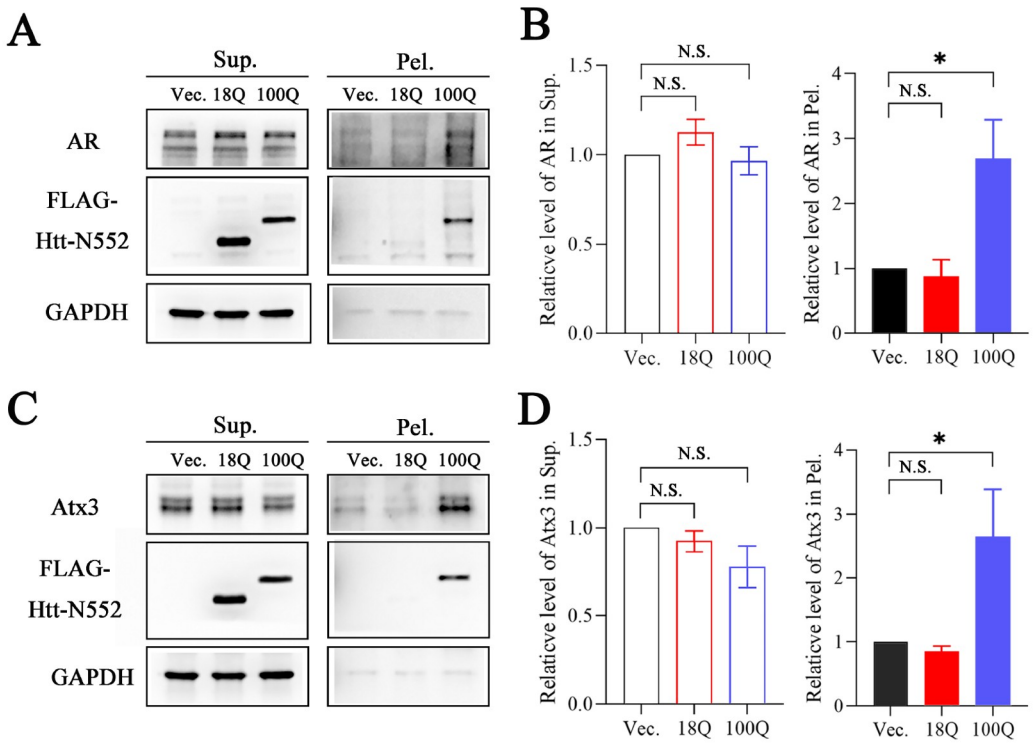

Figure 2. The PQE Htt fragment sequesters endogenous AR and Atx3 into insoluble aggregates (A,C) Supernatant/pellet fractionation for detecting sequestration of endogenous AR (A) and Atx3 (C) by Htt_{100Q}-N552. HEK 293T cells were transfected with empty vector, FLAG-Htt_{18Q}-N552 or FLAG-Htt_{100Q}-N552. Approximately 48 h after transfection, the cell lysates were subject to supernatant/pellet fractionation and then to western blot analysis with an anti-FLAG, anti-AR or anti-Atx3 antibody. (B,D) Quantification of the protein levels of AR (B) and Atx3 (D) in supernatant and pellet fractions. Data are shown as the mean ± SEM ($n = 3$). *$P < 0.05$; N.S., no significance. Vec., vector; Sup., supernatant; Pel., pellet.

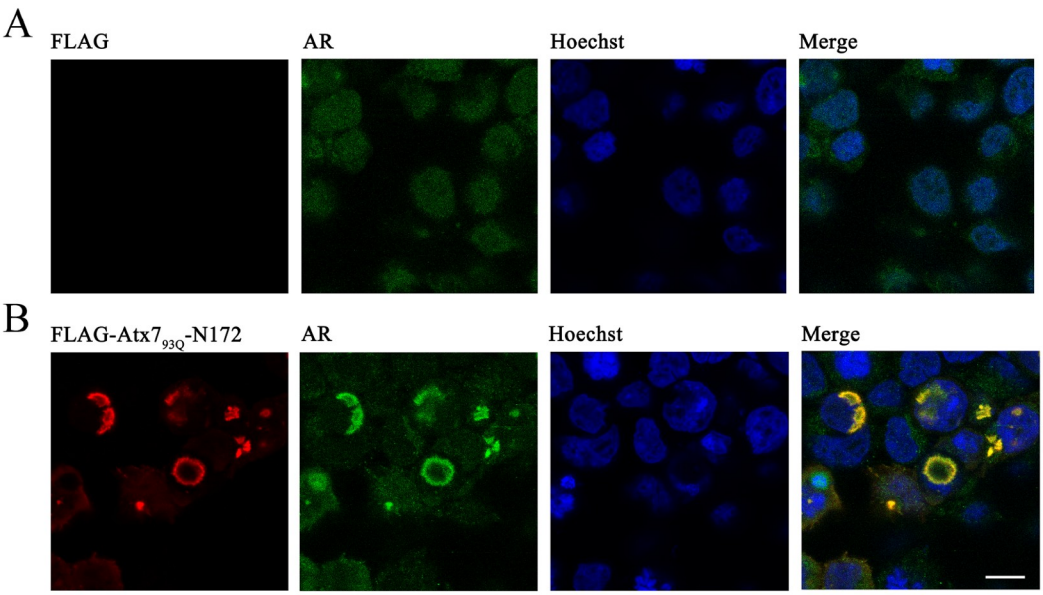

Figure 3. Immunofluorescence images showing sequestration of endogenous AR into inclusions by the PQE Atx7 fragment in cells (A) Vector control. (B) $Atx7_{93Q}$-N172. HEK 293T cells were transfected with the FLAG-$Atx7_{93Q}$-N172 plasmid or control vector and then subjected to confocal microscopic imaging. $Atx7_{93Q}$-N172 and endogenous AR were stained with an anti-FLAG (red) or anti-AR antibody (green), and nuclei were stained with Hoechst (blue). Scale bar: 10 μm.

supernatant and pellet fractions from the aggregated mixtures. Before incubation (0 h), most of the proteins remained in the supernatant, while no coprecipitation occurred. After incubation for 48 h, both $Atx3_{22Q}$-IIC and $Atx3_{6Q}$-IIC could be sequestered into the aggregates formed by $Atx7_{33Q}$-N62 but with different efficiencies (Figure 7). The amount of $Atx3_{22Q}$-IIC (Figure 7B) sequestered into

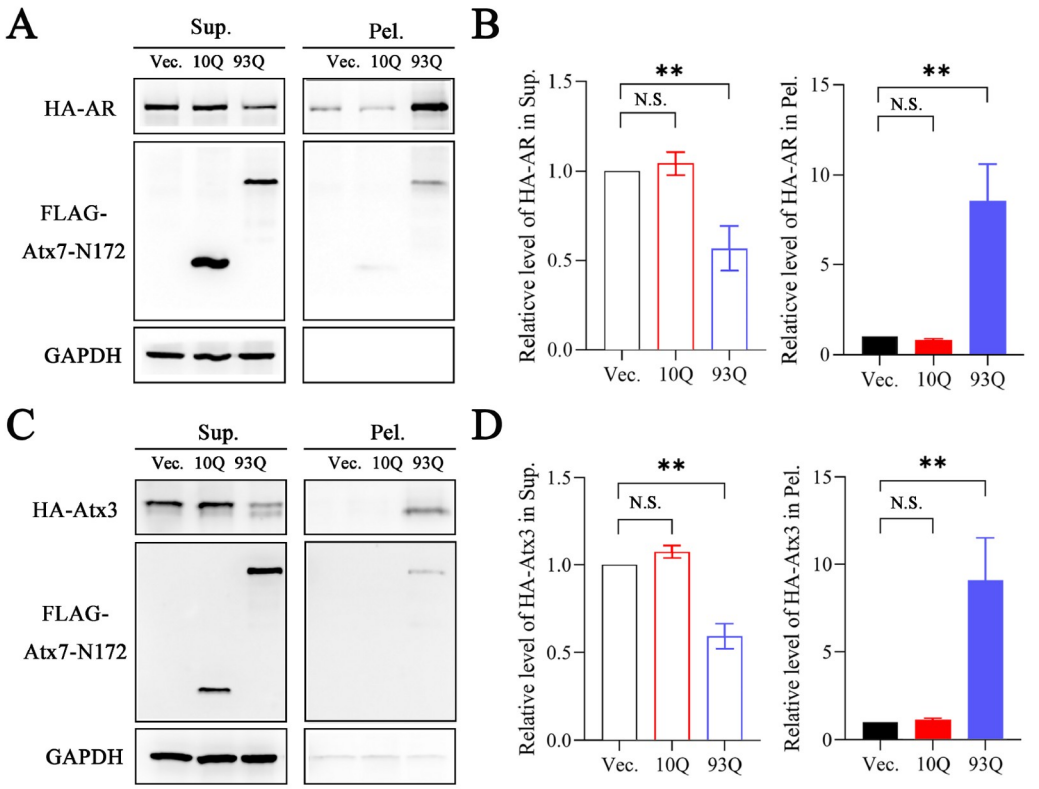

Figure 4. The PQE Atx7 fragment sequesters exogenous AR and Atx3 into aggregates (A,C) Supernatant/pellet fractionation for detecting sequestration of exogenous AR (A) and Atx3 (C) by Atx7$_{93Q}$-N172. HA-AR or HA-Atx3 was cotransfected with FLAG-tagged Atx7$_{10Q}$-N172 or Atx7$_{93Q}$-N172 into HEK 293T cells. Approximately 48 h after transfection, the cell lysates were subject to supernatant/pellet fractionation and then to western blot analysis with an anti-FLAG or anti-HA antibody. (B,D) Quantification of the protein levels of AR (B) and Atx3 (D) in supernatant and pellet fractions. Data are shown as the mean ± SEM ($n = 3$). $^{**}P < 0.01$; N.S., no significance. Vec., vector; Sup., supernatant; Pel., pellet.

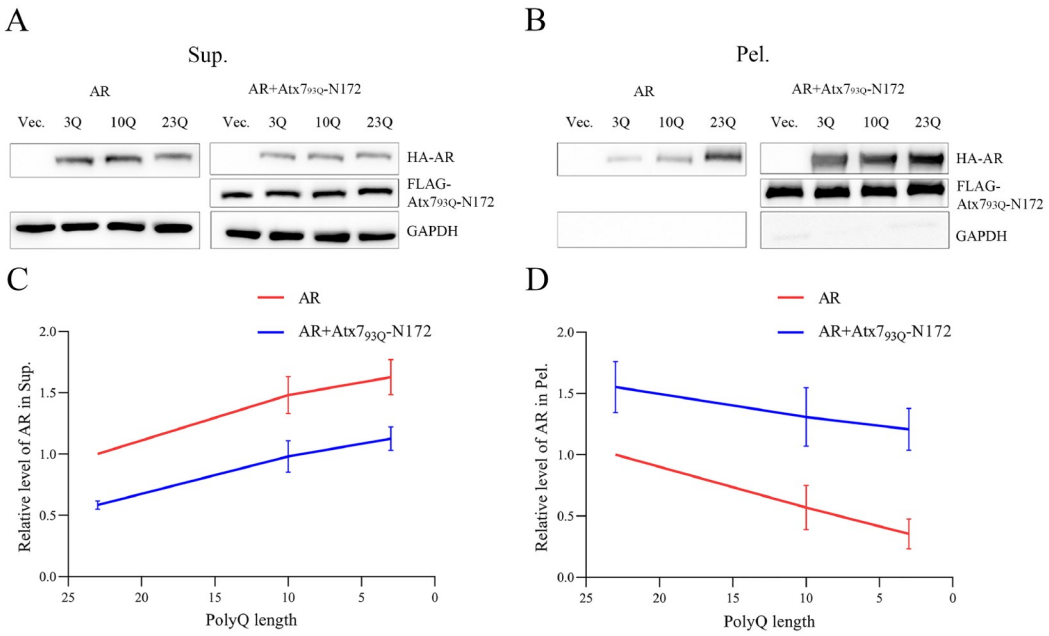

Figure 5. Effect of polyQ length on the sequestration of AR by the PQE Atx7 fragment (A,B) Supernatant/pellet fractionation for characterizing the sequestration effects of AR with different polyQ lengths. FLAG-Atx7$_{93Q}$-N172 was cotransfected with HA-AR (23Q, 10Q or 3Q) into HEK 293T cells. Approximately 48 h after transfection, the cell lysates were subject to supernatant/pellet fractionation and western blot analysis with an anti-FLAG or anti-HA antibody. (C,D) Plots of the relative protein level of AR in supernatant (C) or in pellet (D) versus polyQ length. Data are shown as the mean ± SEM ($n = 3$). 23Q, normal polyQ length of AR; 10Q, AR$_{10Q}$; 3Q, AR$_{3Q}$; Vec., vector; Sup., supernatant; Pel., pellet.

the pellet fraction was larger than that of Atx3$_{6Q}$-IIC (Figure 7A). Simultaneously, the amount of Atx7$_{33Q}$-N62 aggregates was considerably increased with the precipitation of Atx3$_{22Q}$-IIC (Figure 7B), again demonstrating the synergistic coaggregation process between both polyQ proteins (Figures 5 and 6). We also repeated the coprecipitation experiment on Atx3$_{46Q}$-IIC with normal (10Q) or PQE (22Q) Atx7-N62. Similarly, sequestration of Atx7$_{22Q}$-N62 by the Atx3$_{46Q}$-IIC aggregates was more efficient than that of Atx7$_{10Q}$-N62. Thus, the data from *in vitro* coprecipitation indicate that the sequestration effect is polyQ-length dependent, further demonstrating that the heterologous polyQ proteins can coaggregate with each other through polyQ-tract interactions.

PolyQ-polyQ interactions as revealed by NMR titration

To further demonstrate that the coaggregation of polyQ proteins is mediated by polyQ-polyQ interactions, we performed NMR titration of ^{15}N-labelled Atx7$_{22Q}$-N62 with unlabelled Atx3$_{22Q}$-IIC, both of which did not form protein aggregates in solution. We previously partially assigned the backbone chemical shifts of Atx7$_{22Q}$-N62 (T3N9) and characterized the α-helical structure formation around its Ala-rich region 2 (ARR2) and extending to the polyQ tract [49]. The HSQC spectra showed that when titrated with Atx3$_{22Q}$-IIC, some resonance peaks of Atx7$_{22Q}$-N62, such as A23, T32, N38 and T58, became weak gradually but without chemical shift changes (Figure 8A), suggesting that these two polyQ proteins interact with each

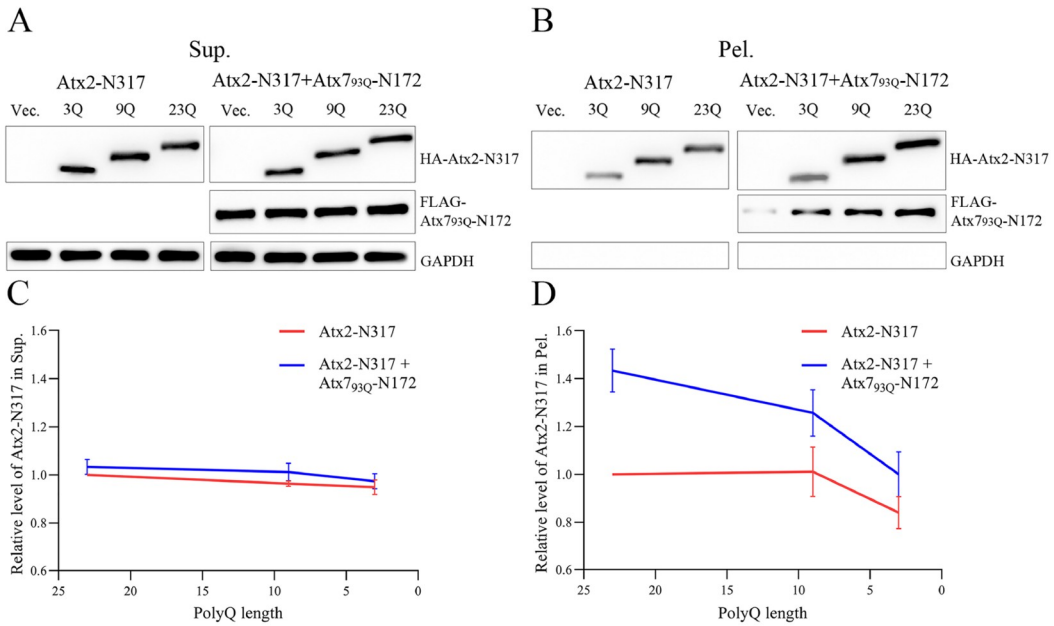

Figure 6. Sequestration by the PQE Atx7 fragment is dependent on the polyQ length of Atx2-N317 (A,B) Supernatant/pellet fractionation for characterizing the sequestration effects of Atx2-N317 with different polyQ lengths. FLAG-Atx7$_{93Q}$-N172 was cotransfected with HA-Atx2-N317 (23Q, 9Q or 3Q) into HEK 293T cells. Approximately 48 h after transfection, the cell lysates were subject to supernatant/pellet fractionation and western blot analysis with an anti-FLAG or anti-HA antibody. (C,D) Plots of the relative protein level of Atx2-N317 in supernatant (C) or in pellet (D) versus polyQ length. Data are shown as the mean ± SEM (n = 3). 23Q, normal polyQ length of the Atx2-N317 fragment; 9Q, Atx2$_{9Q}$-N317; 3Q, Atx2$_{3Q}$-N317; Vec., vector; Sup., supernatant; Pel., pellet.

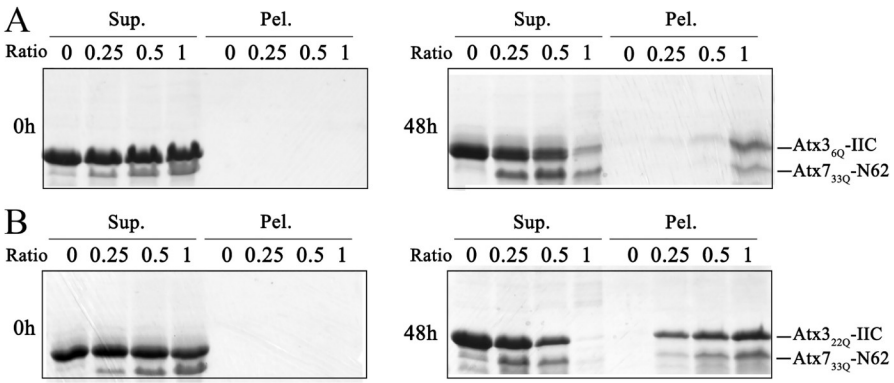

Figure 7. Coprecipitation of Atx7$_{33Q}$-N62 with Atx3-IIC *in vitro* (A) Atx7$_{33Q}$-N62 with Atx3$_{6Q}$-IIC. (B) Atx7$_{33Q}$-N62 with Atx3$_{22Q}$-IIC. The protein mixtures were incubated for 48 h and subject to supernatant/pellet fractionation and SDS-PAGE (15% gel). The concentration of Atx3$_{6Q}$-IIC or Atx3$_{22Q}$-IIC was set as 50 μM, and the molar ratios of Atx7$_{33Q}$-N62/Atx3-IIC were 0.0, 0.25, 0.5 and 1.0. Atx7-N62, the N-terminal fragment (residues 1–62) of Atx7; Atx3-IIC, the C-terminal fragment (residues 221–373) of isoform-II Atx3. Sup., supernatant; Pel., pellet.

other directly but rather weakly. Some Gln residues, including Q30 and Q33 and the unassigned Gln residues (referred to as Qn1, Qn2 and Qn3), were significantly perturbed in peak intensities during titration. The intensity weakening at the N- and C-termini of $Atx7_{22Q}$-N62 upon titration may arise from a tumbling change in the overall protein molecule due to the N/C-terminal flexibilities, which are irrelevant to the interaction sites. Collectively, except for the residues in both termini, most residues with reduced peak intensities resided in the region preceding ARR2 or in the polyQ-tract sequence (Figure 8B). These NMR data indicate that direct polyQ-polyQ interactions may occur between the heterologous polyQ proteins in solution, which may provide the driving force for coaggregation of the polyQ proteins.

PQE fragments suppress the transactivation function of AR

Aggregation of PQE proteins can cause a significant decrease in the protein level of AR in the supernatant and an increase in the aggregated fraction. The dramatic reduction in the soluble and functionally available fractions is likely to cause the loss of normal function of AR in cells. To confirm this hypothesis, we examined the effects of the PQE protein fragments on the transactivation function of AR by a luciferase reporter assay [54]. We prepared a pGL3-ARE plasmid and cotransfected it with different Atx7-N172 species (10Q, 93Q) into HEK 293T cells and then measured the luciferase activities. When the cells were transfected with pGL3-ARE, the fluorescence intensity was significantly enhanced, indicating that luciferase expression was induced by endogenous AR. When cotransfected with $Atx7_{10Q}$-N172, the fluorescence was almost unchanged compared with transfection with pGL3-ARE only, indicating that $Atx7_{10Q}$-N172 has little effect on luciferase expression and activity. Interestingly, the fluorescence intensity of the experimental group cotransfected with $Atx7_{93Q}$-N172 was reduced by approximately 50% compared to that of the $Atx7_{10Q}$-N172 group (Figure 9A). This suggests that PQE Atx7-N172 inhibits the transactivation function of AR by coaggregating with the transcription factor. We also repeated the experiment on AR with PQE Htt-N552, another N-terminal fragment of Htt (residues 1–552). Consistent with $Atx7_{93Q}$-N172 above and the N-terminal Htt in yeast [41], Htt_{100Q}-N552 rather than Htt_{18Q}-N552 caused a dramatic reduction in luciferase activity by suppressing AR function (Figure 9B). As AR is a steroid-activated transcription factor, we also performed an experiment under the condition of AR activation by dihydrotestosterone (DHT). Compared with the control, DHT significantly enhanced luciferase expression and thus its activity by activating endogenous AR (Figure 9C,D). Similarly, the normal polyQ forms had little effect on fluorescence, whereas their PQE forms ($Atx7_{93Q}$-N172 and Htt_{100Q}-N552) affected transactivation by coaggregating with endogenous AR and thus significantly reduced luciferase expression and activity. Together, the luciferase reporter assay demonstrates that PQE proteins can downregulate the transactivation function of AR. This implies that sequestration of AR by PQE protein aggregates may influence the cellular availability of the transcription activator and consequently impair its transactivation function in cells.

Discussion

Protein misfolding and aggregation can lead to cytotoxicity or neurodegeneration, but for a long time, its pathological mechanism remains disputable. The recruitment/sequestration model states that sequestration of cellular interacting partners by protein aggregates is implicated in the loss-of-function pathologies of NDs [16]. This study demonstrates that PQE Atx7 or Htt coaggregates with AR and Atx3 and sequesters them into insoluble aggregates or inclusions. Sequestration of endogenous AR and other polyQ proteins via a coaggregation process can lead to depletion of their cellular availabilities and cause loss of normal functions (Figure 10). AR is a transcription factor with a polyQ tract; it can be sequestered into inclusions through polyQ-tract interactions, which may cause loss of its cellular availability and transcriptional function. Therefore, it is deduced that PQE proteins can also sequester other essential transcription factors (such as TBP and CBP), deprive their cellular availabilities and functionalities, and consequently impair cellular proteostasis networks.

Coaggregation may occur among diverse amyloidogenic proteins, such as polyQ proteins [14,42,44,47], amyloid-β peptide [56,57] and α-synuclein [58–60]. When a PQE protein forms aggregates in cells, it will coaggregate with other polyQ proteins and sequester them into insoluble inclusions. A polyQ-containing fragment often coaggregates with the full-length protein and suppresses its normal function [34,36,41]. Our present study reveals that the PQE fragment of Atx7 or Htt coaggregates heterologously with endogenous AR and Atx3. This coaggregation effect may cause partial depletion of Atx3 functionality [61] and suppression of the transactivation function of AR (Figure 9). It should be noted that in this study, we performed exogenous overexpression of PQE Atx7 and Htt fragments in a cell model to demonstrate that PQE proteins coaggregate with endogenous proteins (AR, Atx3, *etc.*) and impair their cellular proteostasis. Stable cell lines (*e.g.*, knock-in of PQE fragments) or animal models should be applied to further prove the biological significance. Collectively, coaggregation among polyQ proteins may cause depletion of their cellular availabilities and consequently lead to impairment of the cellular proteostasis of biologically vital proteins.

WT polyQ protein normally contains a polyQ tract of approximately 20 glutamine residues; it is not potent enough to self-aggregate in its full length. However, a PQE protein in cells may have an intrinsic propensity to aggregate, and during the aggregation process, it may coaggregate with other polyQ proteins and sequester them into aggregates or inclusions. A possible explanation is that the promiscuity of polyQ aggregates is beneficial to cross-seeding with any other polypeptide chains, which may be the structural bases for polyQ coaggregation. Our study suggests that the coaggregation of polyQ proteins is probably mediated by polyQ-tract interactions. Similar *in vitro* studies have demonstrated that polyQ peptides can self-aggregate and sequester heterologous polyQ peptides in a polyQ length-dependent manner [62], and the peptide chains generally adopt cross β-sheet structures in fibrillar aggregates [63,64]. These findings strongly support the sequestration model, in which cellular proteins with normal polyQ lengths may be deprived of their functional availabilities when they are sequestered into aggregates formed by a PQE protein. During aggregation of the PQE protein in cells, it may coaggregate with other endogenous polyQ proteins, sequester them into amyloid inclusions, and thus impair their cellular proteostasis. Thus, coaggregation may occur among the nine pathogenic polyQ proteins yet identified [4,14] and probably with nonpathogenic polyQ-containing proteins, such as CBP [42,43,45,46] and transcription factor EB (TFEB) [65]. In

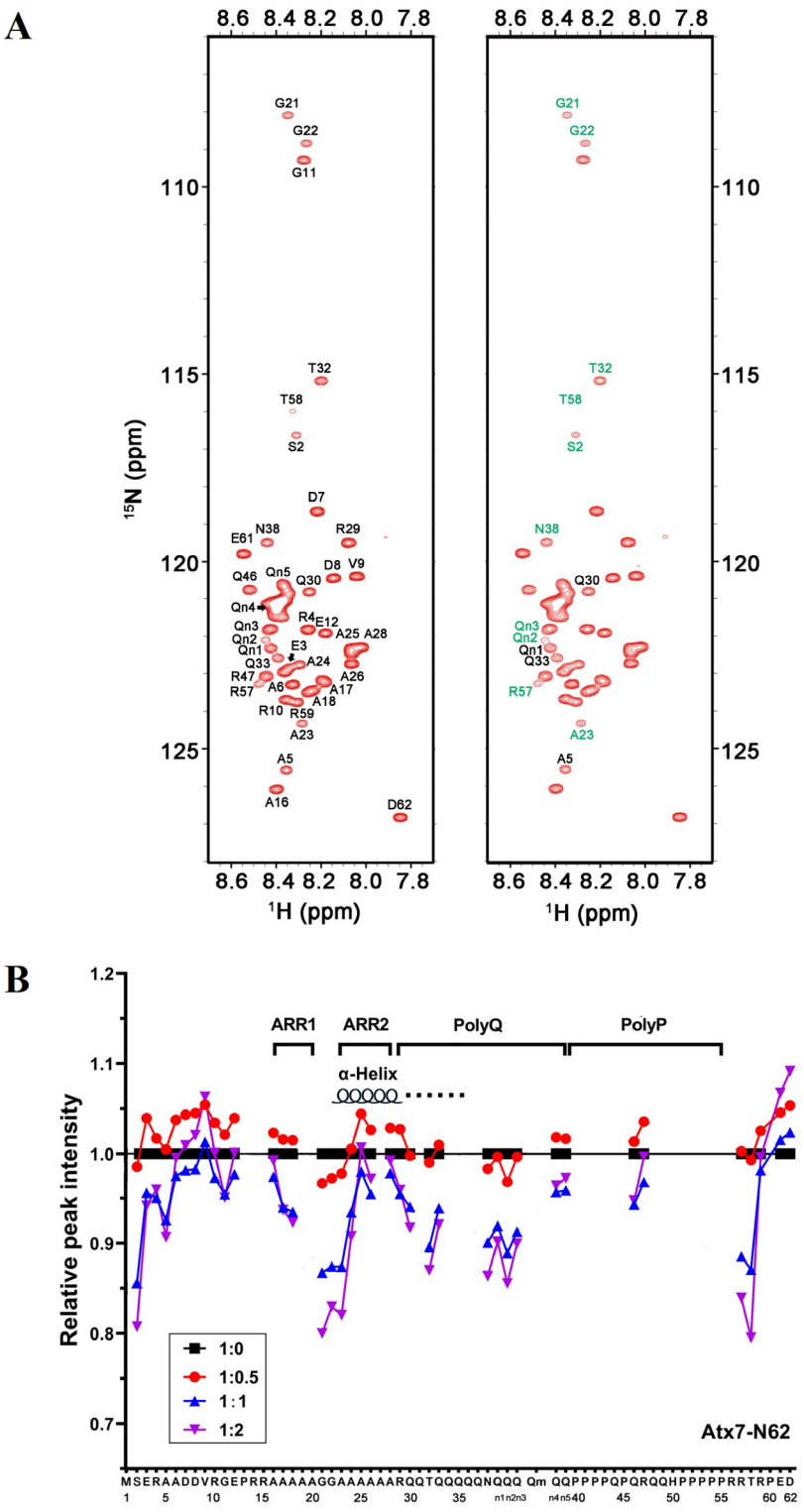

Figure 8. NMR titration for detecting weak interactions between polyQ proteins (A) HSQC spectrum of 15N-labelled Atx7$_{22Q}$-N62(T3N9) with (right) or without the addition of Atx3$_{22Q}$-IIC at a molar ratio of 1:2. The residues with peak intensity changes greater than 10% are marked with green, while those greater than 8% are marked with black. (B) Plot of the relative amide peak intensity against the residue number of Atx7$_{22Q}$-N62 (T3N9) in titration with Atx3$_{22Q}$-IIC. The ratios of [Atx7$_{22Q}$-N62(T3N9)]/[Atx3$_{22Q}$-IIC] were 1: 0 (black), 1: 0.5 (red), 1: 1 (blue) and 1: 2 (purple). The peak intensities (heights) were normalized as 1 for all peaks of 15N-Atx7$_{22Q}$-N62(T3N9) only (1: 0). The average of the intensities was ~0.94 (94%) at a 1:2 ratio titration.

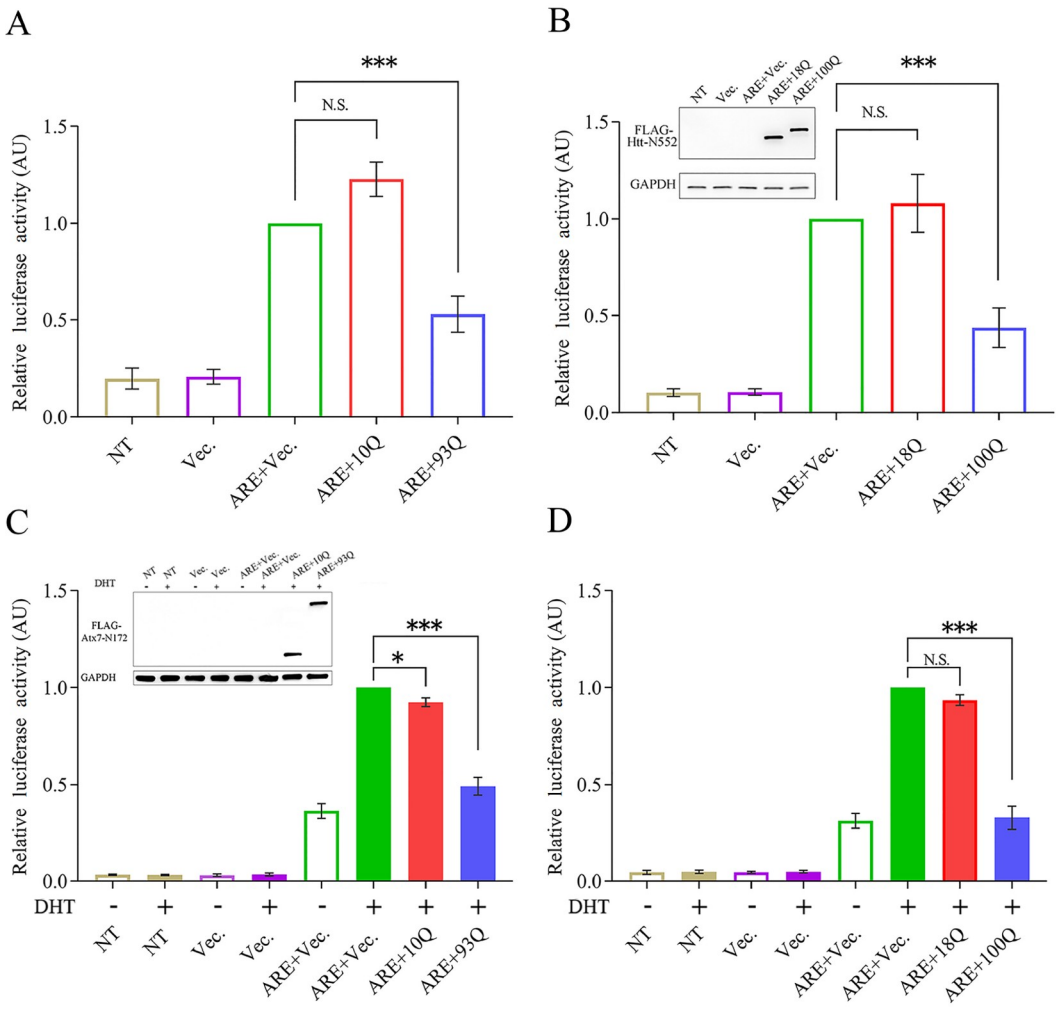

Figure 9. Luciferase reporter assay showing that the fragments of PQE Atx7 and Htt impair the transactivation function of AR (A) Effect of $Atx7_{93Q}$-N172 on the luciferase activity mediated by endogenous AR. The pGL3-ARE plasmid was cotransfected with FLAG-tagged $Atx7_{10Q}$-N172 or $Atx7_{93Q}$-N172 into HEK 293T cells, and the cell lysates were subject to a luciferase activity assay. The empty vector was used as a control. (B) Effect of Htt_{100Q}-N552. FLAG-tagged Htt_{18Q}-N552 and Htt_{100Q}-N552 were applied. Inset: the cell lysates (100 μL) were also analyzed by western blot analysis to indicate equivalent loading of Htt-N552. (C) As in (A), effect of $Atx7_{93Q}$-N172 under the condition of DHT activation. Inset: equivalent loading of Atx7-N172. (D) As in (B), effect of Htt_{100Q}-N552 under the condition of DHT activation. Data are shown as the mean ± SEM ($n = 3$). *$P < 0.05$; ***$P < 0.001$; N.S., no significance. NT, nontransfected; Vec., vector; ARE, pGL3-ARE plasmid; 10Q, $Atx7_{10Q}$-N172; 93Q, $Atx7_{93Q}$-N172; 18Q, Htt_{18Q}-N552; 100Q, Htt_{100Q}-N552.

addition, polyQ aggregates can also colocalize with TDP-43 in cells and sequester this pathogenic protein into inclusions [66,67]. Considering the existence of the glutamine/asparagine (Q/N)-rich region (31% Q/N content) in the C-terminus of TDP-43, it is rational to deduce that coaggregation is mediated by direct interaction of the polyQ tract with the Q/N-rich region of TDP-43 [66]. Other RNA-binding proteins containing a Q/N-rich region, such as TIA1 and FUS/TLS, have also been reported to colocalize with polyQ aggregates in cells [66,68]. Similar research in yeast has also suggested that the Q/N-rich region of Sup35 plays an important role in the coaggregation of polyQ-related proteins [69].

Schiffer *et al.* [41] reported that in a yeast model, the transactivation function of exogenous AR can be inhibited by its own N-terminal PQE fragments, in which the soluble polyQ-containing oligomers rather than the insoluble aggregates bind to the full-length AR and inactivate its function. In this study, we further demonstrate that the transactivation function of endogenous AR can be suppressed heterologously by a fragment of PQE Atx7 or Htt in a human cell line. The endogenous AR contains a polyQ tract of normal length in its N-terminus that may mediate coaggregation with other PQE proteins and sequestration by the polyQ aggregates. Once AR accumulates in the polyQ aggregates, its available amounts or functional fractions will be obviously decreased. Thus, depletion and impairment of the endogenous polyQ proteins of cellular essential functions, such as AR and Atx3, could be a possible mechanism underlying cytotoxicities or neurodegeneration caused by polyQ-protein aggregation. It is rational to deduce that a PQE protein or fragment in patients would interact mutually with other polyQ proteins and combine actions in the pathogenic progression of the disease, which is also implicated in the copathologies of various neurodegenerative diseases [70,71]. Therefore, accumulation of heterologous polyQ proteins in

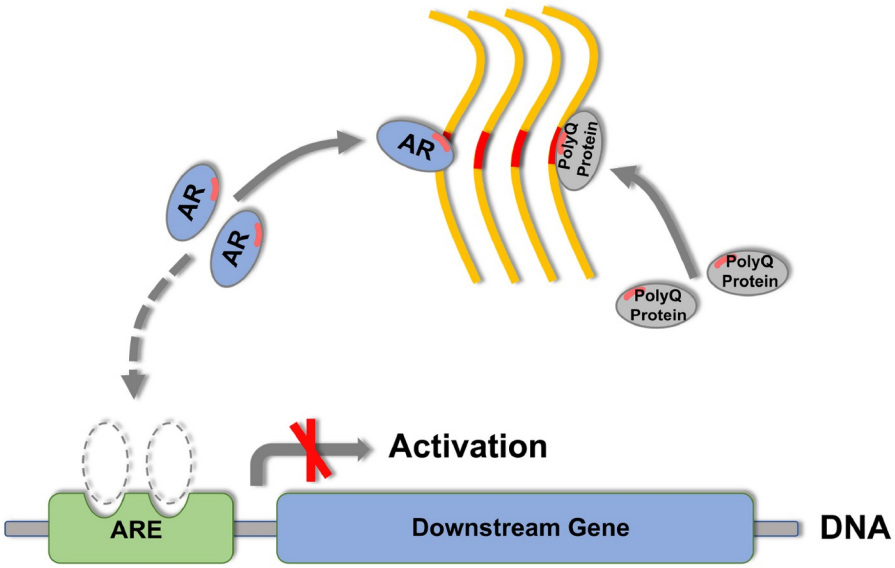

Figure 10. Schematic representation of the coaggregation of polyQ proteins and the consequent impairment of cellular proteostasis The PQE protein forms fibrillar aggregates (yellow), coaggregates with endogenous AR (blue) and/or other polyQ proteins (gray) through their polyQ tracts and sequesters them into insoluble aggregates or inclusions. These coaggregation and sequestration processes may significantly influence the cellular availability of the sequestered polyQ proteins and consequently impair their cellular proteostasis networks, *e.g.*, suppressing the transactivation function of AR and retarding its downstream gene expression. The polyQ tracts in AR and other polyQ proteins are highlighted in red bars. ARE (green), androgen responsive element.

inclusions might be one of the pathogenic causes of polyQ diseases.

Acknowledgement

The authors would like to thank the technicians in the Nuclear Magnetic Resonance System at the National Center for Protein Science in Shanghai, Zhangjiang Laboratory (NFPS, ZJLab), China for providing technical support and assistance in data collection and analysis. We also thank Drs. Jiang-Ye Chen and Hui Yang for constructive discussion and valuable suggestions, and Drs. Wei Xue and Wen-Tian He for technical help.

Funding

This work was supported by the grants from the National Natural Science Foundation of China (Nos. 31470758 and 31870764).

Conflict of Interest

The authors declare that they have no conflict of interest.

References

1. Chiti F, Dobson C.M. Protein misfolding, amyloid formation, and human disease: a summary of progress over the last decade. *Annu Rev Biochem* 2017, 86: 27–68
2. Hartl FU. Protein misfolding diseases. *Annu Rev Biochem* 2017, 86: 21–26
3. Adegbuyiro A, Sedighi F, Pilkington Iv AW, Groover S, Legleiter J. Proteins containing expanded polyglutamine tracts and neurodegenerative disease. *Biochemistry* 2017, 56: 1199–1217
4. Orr HT, Zoghbi HY. Trinucleotide repeat disorders. *Annu Rev Neurosci* 2007, 30: 575–621
5. Lieberman AP, Shakkottai VG, Albin RL. Polyglutamine repeats in neurodegenerative diseases. *Annu Rev Pathol Mech Dis* 2019, 14: 1–27
6. Cox D, Raeburn C, Sui X, Hatters DM. Protein aggregation in cell biology: An aggregomics perspective of health and disease. *Semin Cell Dev Biol* 2020, 99: 40–54
7. Kumar V, Sami N, Kashav T, Islam A, Ahmad F, Hassan MI. Protein aggregation and neurodegenerative diseases: From theory to therapy. *Eur J Medicinal Chem* 2016, 124: 1105–1120
8. Li H, Li SH, Yu ZX, Shelbourne P, Li XJ. Huntingtin aggregate-associated axonal degeneration is an early pathological event in huntington's disease mice. *J Neurosci* 2001, 21: 8473–8481
9. McLoughlin HS, Moore LR, Paulson HL. Pathogenesis of SCA3 and implications for other polyglutamine diseases. *Neurobiol Dis* 2020, 134: 104635
10. Dugger BN, Dickson DW. Pathology of neurodegenerative diseases. *Cold Spring Harb Perspect Biol* 2017, 9: a028035
11. Donaldson KM, Li W, Ching KA, Batalov S, Tsai CC, Joazeiro CAP. Ubiquitin-mediated sequestration of normal cellular proteins into polyglutamine aggregates. *Proc Natl Acad Sci USA* 2003, 100: 8892–8897
12. Zeng L, Wang B, Merillat SA, Minakawa EN, Perkins MD, Ramani B, Tallaksen-Greene SJ, *et al.* Differential recruitment of UBQLN2 to nuclear inclusions in the polyglutamine diseases HD and SCA3. *Neurobiol Dis* 2015, 82: 281–288
13. Yang H, Liu S, He WT, Zhao J, Jiang LL, Hu HY. Aggregation of polyglutamine-expanded ataxin 7 protein specifically sequesters ubiquitin-specific protease 22 and deteriorates its deubiquitinating function in the spt-ada-gcn5-acetyltransferase (SAGA) complex. *J Biol Chem* 2015, 290: 21996–22004
14. Perez MK, Paulson HL, Pendse SJ, Saionz SJ, Bonini NM, Pittman RN. Recruitment and the role of nuclear localization in polyglutamine-mediated aggregation. *J Cell Biol* 1998, 143: 1457–1470
15. Satyal SH, Schmidt E, Kitagawa K, Sondheimer N, Lindquist S, Kramer JM, Morimoto RI. Polyglutamine aggregates alter protein folding homeostasis in *Caenorhabditis elegans*. *Proc Natl Acad Sci USA* 2000, 97: 5750–5755
16. Yang H, Hu H-. Sequestration of cellular interacting partners by protein aggregates: implication in a loss-of-function pathology. *FEBS J* 2016, 283:

3705–3717
17. Jiang H, Poirier MA, Liang Y, Pei Z, Weiskittel CE, Smith WW, DeFranco DB, *et al.* Depletion of CBP is directly linked with cellular toxicity caused by mutant huntingtin. *Neurobiol Dis* 2006, 23: 543–551
18. Yue HW, Hu HY. Sequestration of cellular essential proteins or RNA by polyglutamine-expanded protein aggregates. *Prog Biochem Biophy* 2018, 45: 1204–1213
19. Ano Bom APD, Rangel LP, Costa DCF, de Oliveira GAP, Sanches D, Braga CA, Gava LM, *et al.* Mutant p53 aggregates into prion-like amyloid oligomers and fibrils. *J Biol Chem* 2012, 287: 28152–28162
20. Silva JL, Gallo CVDM, Costa DCF, Rangel LP. Prion-like aggregation of mutant p53 in cancer. *Trends Biochem Sci* 2014, 39: 260–267
21. de Oliveira GAP, Petronilho EC, Pedrote MM, Marques MA, Vieira TCRG, Cino EA, Silva JL. The status of p53 oligomeric and aggregation states in cancer. *Biomolecules* 2020, 10: 548
22. Xu J, Reumers J, Couceiro JR, De Smet F, Gallardo R, Rudyak S, Cornelis A, *et al.* Gain of function of mutant p53 by coaggregation with multiple tumor suppressors. *Nat Chem Biol* 2011, 7: 285–295
23. Ellerby LM, Hackam AS, Propp SS, Ellerby HM, Rabizadeh S, Cashman NR, Trifiro MA, *et al.* Kennedy's disease: caspase cleavage of the androgen receptor is a crucial event in cytotoxicity. *J NeuroChem* 1999, 72: 185–195
24. Berke SJS, Schmied FAF, Brunt ER, Ellerby LM, Paulson HL. Caspase-mediated proteolysis of the polyglutamine disease protein ataxin-3. *J Neurochem* 2004, 89: 908–918
25. Wellington CL, Singaraja R, Ellerby L, Savill J, Roy S, Leavitt B, Cattaneo E, *et al.* Inhibiting caspase cleavage of huntingtin reduces toxicity and aggregate formation in neuronal and nonneuronal cells. *J Biol Chem* 2000, 275: 19831–19838
26. Matos C.A, Almeida L.P, Nobrega C. Proteolytic cleavage of polyglutamine disease-causing proteins: revisiting the toxic fragment hypothesis. *Curr Pharm Des* 2017, 23: 753–775
27. Niewiadomska-Cimicka A, Hache A, Trottier Y. Gene deregulation and underlying mechanisms in spinocerebellar ataxias with polyglutamine expansion. *Front Neurosci* 2020, 14: 571
28. Graham RK, Deng Y, Slow EJ, Haigh B, Bissada N, Lu G, Pearson J, *et al.* Cleavage at the caspase-6 site is required for neuronal dysfunction and degeneration due to mutant huntingtin. *Cell* 2006, 125: 1179–1191
29. Graham RK, Deng Y, Carroll J, Vaid K, Cowan C, Pouladi MA, Metzler M, *et al.* Cleavage at the 586 amino acid caspase-6 site in mutant huntingtin influences caspase-6 activation *in vivo*. *J Neurosci* 2010, 30: 15019–15029
30. Landles C, Sathasivam K, Weiss A, Woodman B, Moffitt H, Finkbeiner S, Sun B, *et al.* Proteolysis of mutant huntingtin produces an exon 1 fragment that accumulates as an aggregated protein in neuronal nuclei in Huntington disease. *J Biol Chem* 2010, 285: 8808–8823
31. Garden GA, Libby RT, Fu YH, Kinoshita Y, Huang J, Possin DE, Smith AC, *et al.* Polyglutamine-expanded ataxin-7 promotes non-cell-autonomous purkinje cell degeneration and displays proteolytic cleavage in ataxic transgenic mice. *J Neurosci* 2002, 22: 4897–4905
32. Guyenet SJ, Mookerjee SS, Lin A, Custer SK, Chen SF, Sopher BL, La Spada AR, *et al.* Proteolytic cleavage of ataxin-7 promotes SCA7 retinal degeneration and neurological dysfunction. *Hum Mol Genet* 2015, 24: 3908–3917
33. Young JE, Gouw L, Propp S, Sopher BL, Taylor J, Lin A, Hermel E, *et al.* Proteolytic cleavage of ataxin-7 by caspase-7 modulates cellular toxicity and transcriptional dysregulation. *J Biol Chem* 2007, 282: 30150–30160
34. Haacke A, Broadley SA, Boteva R, Tzvetkov N, Hartl FU, Breuer P. Proteolytic cleavage of polyglutamine-expanded ataxin-3 is critical for aggregation and sequestration of non-expanded ataxin-3. *Hum Mol Genet* 2006, 15: 555–568
35. Haacke A, Hartl FU, Breuer P. Calpain inhibition is sufficient to suppress aggregation of polyglutamine-expanded ataxin-3. *J Biol Chem* 2007, 282: 18851–18856
36. Hubener J, Weber JJ, Richter C, Honold L, Weiss A, Murad F, Breuer P, *et al.* Calpain-mediated ataxin-3 cleavage in the molecular pathogenesis of spinocerebellar ataxia type 3 (SCA3). *Hum Mol Genet* 2013, 22: 508–518
37. Simoes AT, Goncalves N, Koeppen A, Deglon N, Kugler S, Duarte CB, Pereira de Almeida L. Calpastatin-mediated inhibition of calpains in the mouse brain prevents mutant ataxin 3 proteolysis, nuclear localization and aggregation, relieving Machado-Joseph disease. *Brain* 2012, 135: 2428–2439
38. Estebanez-Perpina E, Moore JMR, Mar E, Delgado-Rodrigues E, Nguyen P, Baxter JD, Buehrer BM, *et al.* The molecular mechanisms of coactivator utilization in ligand-dependent transactivation by the androgen receptor. *J Biol Chem* 2005, 280: 8060–8068
39. Chen JF, Lin PW, Tsai YR, Yang YC, Kang HY. Androgens and androgen receptor actions on bone health and disease: from androgen deficiency to androgen therapy. *Cells* 2019, 8: 1318
40. Gelmann EP. Molecular biology of the androgen receptor. *J Clin Oncol* 2002, 20: 3001–3015
41. Schiffer NW, Céraline J, Hartl FU, Broadley SA. N-terminal polyglutamine-containing fragments inhibit androgen receptor transactivation function. *Biol Chem* 2008, 389: 1455–1466
42. Nucifora F.C Jr, Sasaki M, Peters MF, Huang H, Cooper JK, Yamada M, Takahashi H, *et al.* Interference by huntingtin and atrophin-1 with cbp-mediated transcription leading to cellular toxicity. *Science* 2001, 291: 2423–2428
43. Jiang H. Cell death triggered by polyglutamine-expanded huntingtin in a neuronal cell line is associated with degradation of CREB-binding protein. *Hum Mol Genet* 2003, 12: 1–12
44. Chai Y, Shao J, Miller VM, Williams A, Paulson HL. Live-cell imaging reveals divergent intracellular dynamics of polyglutamine disease proteins and supports a sequestration model of pathogenesis. *Proc Natl Acad Sci USA* 2002, 99: 9310–9315
45. McCampbell A, *et al.* CREB-binding protein sequestration by expanded polyglutamine. *Hum Mol Genet* 2000, 9: 2197–2202
46. Chai Y, Wu L, Griffin JD, Paulson HL. The role of protein composition in specifying nuclear inclusion formation in polyglutamine disease. *J Biol Chem* 2001, 276: 44889–44897
47. Huang CC, Faber PW, Persichetti F, Mittal V, Vonsattel JP, MacDonald ME, Gusella JF. Amyloid formation by mutant huntingtin: threshold, progressivity and recruitment of normal polyglutamine proteins. *Somat Cell Mol Genet* 1998, 24: 217–233
48. Lee J, Kim M, Itoh TQ, Lim C. Ataxin-2: a versatile posttranscriptional regulator and its implication in neural function. *WIREs RNA* 2018, 9: e1488
49. Hong JY, Wang DD, Xue W, Yue HW, Yang H, Jiang LL, Wang WN, *et al.* Structural and dynamic studies reveal that the Ala-rich region of ataxin-7 initiates α-helix formation of the polyQ tract but suppresses its aggregation. *Sci Rep* 2019, 9: 7481
50. Yang H, Li JJ, Liu S, Zhao J, Jiang YJ, Song AX, Hu HY. Aggregation of polyglutamine-expanded ataxin-3 sequesters its specific interacting partners into inclusions: implication in a loss-of-function pathology. *Sci Rep* 2014, 4: 6410
51. Yang H, Yue HW, He WT, Hong JY, Jiang LL, Hu HY. PolyQ-expanded huntingtin and ataxin-3 sequester ubiquitin adaptors hHR23B and UBQLN2 into aggregates *via* conjugated ubiquitin. *FASEB J* 2018, 32: 2923–2933
52. Cleutjens KBJM, van Eekelen CCEM, van der Korput HAGM, Brinkmann

AO, Trapman J. Two androgen response regions cooperate in steroid hormone regulated activity of the prostate-specific antigen promoter. *J Biol Chem* 1996, 271: 6379–6388

53. Azeem W, Hellem MR, Olsen JG, Hua Y, Marvyin K, Qu Y, Lin B, ***et al.*** An androgen response element driven reporter assay for the detection of androgen receptor activity in prostate cells. *PLoS One* 2017, 12: e0177861
54. Solberg, N. and S. Krauss, Luciferase assay to study the activity of a cloned promoter DNA fragment. *Methods Mol Biol*, 2013, 977: 65–78
55. Hakim-Eshed V, Boulos A, Cohen-Rosenzweig C, Yu-Taeger L, Ziv T, Kwon YT, Riess O, ***et al.*** Site-specific ubiquitination of pathogenic huntingtin attenuates its deleterious effects. *Proc Natl Acad Sci USA* 2020, 117: 18661–18669
56. Luo J, Warmlander SKTS, Gräslund A, Abrahams JP. Cross-interactions between the alzheimer disease amyloid-β peptide and other amyloid Proteins: a further aspect of the amyloid cascade hypothesis. *J Biol Chem* 2016, 291: 16485–16493
57. Bondarev S, Antonets K, Kajava A, Nizhnikov A, Zhouravleva G. Protein co-aggregation related to amyloids: methods of investigation, diversity, and classification. *Int J Mol Sci* 2018, 19: 2292
58. Herrera F, Outeiro TF. α-Synuclein modifies huntingtin aggregation in living cells. *FEBS Lett* 2012, 586: 7–12
59. Bhasne K, Mukhopadhyay S. Formation of heterotypic amyloids: α-synuclein in co-aggregation. *Proteomics* 2018, 18: 1800059
60. Vaneyck J, Segers-Nolten I, Broersen K, Claessens MMAE. Cross-seeding of alpha-synuclein aggregation by amyloid fibrils of food proteins. *J Biol Chem* 2021, 296: 100358
61. Yue HW, Hong JY, Zhang SX, Jiang LL, Hu HY. PolyQ-expanded proteins impair cellular proteostasis of ataxin-3 through sequestering the co-chaperone HSJ1 into aggregates. *Sci Rep* 2021, 11: 7815
62. Chen S, Berthelier V, Yang W, Wetzel R. Polyglutamine aggregation behavior *in vitro* supports a recruitment mechanism of cytotoxicity. *J Mol Biol* 2001, 311: 173–182
63. Punihaole D, Workman RJ, Hong Z, Madura JD, Asher SA. Polyglutamine fibrils: new insights into antiparallel β-sheet conformational preference and side chain structure. *J Phys Chem B* 2016, 120: 3012–3026
64. Schneider R, Schumacher MC, Mueller H, Nand D, Klaukien V, Heise H, Riedel D, ***et al.*** Structural characterization of polyglutamine fibrils by solid-state NMR spectroscopy. *J Mol Biol* 2011, 412: 121–136
65. Yang J, Xu H, Zhang C, Yang X, Cai W, Chen X. A prion-like domain of TFEB mediates the co-aggregation of TFEB and mHTT. *Autophagy* 2023, 19: 544–550
66. Fuentealba RA, Udan M, Bell S, Wegorzewska I, Shao J, Diamond MI, Weihl CC, ***et al.*** Interaction with polyglutamine aggregates reveals a Q/N-rich domain in TDP-43. *J Biol Chem* 2010, 285: 26304–26314
67. Coudert L, Nonaka T, Bernard E, Hasegawa M, Schaeffer L, Leblanc P. Phosphorylated and aggregated TDP-43 with seeding properties are induced upon mutant Huntingtin (mHtt) polyglutamine expression in human cellular models. *Cell Mol Life Sci* 2019, 76: 2615–2632
68. Doi H, Okamura K, Bauer PO, Furukawa Y, Shimizu H, Kurosawa M, Machida Y, ***et al.*** RNA-binding protein TLS is a major nuclear aggregate-interacting protein in huntingtin exon 1 with expanded polyglutamine-expressing cells. *J Biol Chem* 2008, 283: 6489–6500
69. Zhao X, Park YN, Todor H, Moomau C, Masison D, Eisenberg E, Greene LE. Sequestration of Sup35 by aggregates of huntingtin fragments causes toxicity of [PSI +] yeast. *J Biol Chem* 2012, 287: 23346–23355
70. Coulthard EJ, Love S. A broader view of dementia: multiple co-pathologies are the norm. *Brain* 2018, 141: 1894–1897
71. Nonaka T, Masuda-Suzukake M, Hasegawa M. Molecular mechanisms of the co-deposition of multiple pathological proteins in neurodegenerative diseases. *Neuropathology* 2018, 38: 64–71